THE BINARY COLLISION APPROXIMATION IN THE THEORY OF LINE BROADENING BY FOREIGN GASES

By E. Czuchaj and J. Fiutak

Institute of Physics, University of Gdańsk*

(Received November 5, 1970)

The shape of the atomic line broadened by foreign gases is examined in the extended binary collision approximation. It is shown that this approximation is applicable, under the normal spectroscopic conditions, in the pressure range up to about ten atmospheres. The dependence of the line shape parameters on the interatomic potential is investigated and the results are presented graphically. It is shown that the present approach may explain the non-linear dependence of the line shift and half-width on the pressure and that the calculated line shape curves reveal a distinct asymmetry for the pressure above one atmosphere.

1. Introduction

In the present paper we wish to continue the discussion of the model of the foreign gas broadening of atomic lines, which we have worked out in the previous paper [1] to be refered here as the paper I. Particularly, we will discuss the various aspects of the binary collision approximation by analyzing some of the methods known from the literature, namely the impact theory, the Anderson-Talman method and the resolvent operator approach.

The essential features of the model adopted in the paper I and in most papers on the pressure broadening may be summarized as follows:

1. The spectral lines do not overlap. 2. The radiating atom is immovable. 3. The interaction between the perturbers is neglected. 4. The coupling between the radiating atom and a perturber is represented, for a definite atomic state, by an interaction potential dependent only on the relative distance.

This model is particularly well suited for the description of the low pressure data on the atomic lines broadening by inert gases. It has the virtue of producing the Fourier conjugate of the intensity distribution function in the following closed form

$$\overline{U}_{if}(t) = \exp\{-in\int_0^t V_{if}(t')\,dt'\}, \tag{1}$$

* Address: Instytut Fizyki, Uniwersytet Gdański, Gdańsk 6, Sobieskiego 18, Poland.

for the spectral line corresponding to the transition of the radiating atom from the initial state i to the final f due to the absorption of light. Let us recall, that the function $V_{if}(t)$, which characterises the interaction between the radiating atom and a given perturber, is defined as follows

$$V_{if}(t) = \Omega Tr \{\varrho(h_i)\, e^{ih_f t}\, (v_i - v_f)\, e^{-ih_i t}\}. \tag{2}$$

Thus the calculation of the function $\overline{U}_{if}(t)$ requires only, at least in principle, the knowledge of the potentials v_i and v_f of the perturber moving in the field of the radiating atom in its initial and final state respectively. Then the intensity distribution function $J_{if}(x)$ is given as the Fourier conjugate of $\overline{U}_{if}(t)$ as follows

$$J_{if}(x) = \frac{1}{2\pi} \int_{-\infty}^{\infty} e^{-ixt} \overline{U}_{if}(t) dt. \tag{3}$$

The program sketched above is known as the Anderson–Talman method which has been successfully applied by Griem and others [2] to the description of atomic lines broadening by the collisions with ions in plasma conditions. However, using this method we do not gain the accuracy adequate to the computational effort involved here, which is rather discouraging even in the classical path approximation so that the numerical calculations presented in the literature are based on the use of some oversimplified models of the interatomic potential.

What we aim at is to show how to improve the line shape calculation, as compared against the impact theory, without a waste of the computer time. Therefore we will divide the range of the pressure, at moderate temperatures, into the low pressure region, which extends up to about one atmosphere, and the intermediate region covering the pressures up to about ten atmospheres. The first is the region where the impact approximation is valid, whereas for the intermediate region our own proposal of the line shape calculation is presented in the fourth section. We do not touch here the problem of the line shape at very low pressures, where the Doppler effect becomes important.

The proposed method of the line shape calculation is justified by the analysis of the intensity distribution on the wings of the line, which is performed in the second section, and the centre-of-line calculation, which is presented in the third section.

The numerical results, which are given in the last section, are in agreement with the experimental results of Ch'en and others [3] concerning the intermediate pressure data on cesium line broadening by inert gases. Those results have shown a nonlinear dependence of the line shape parameters on the pressure and asymmetry of the line profiles for the pressure above one atmosphere.

2. Frequency distribution in the wings region

In the paper I the intensity distribution has been analyzed with the help of the following formulas

$$J_{if}(x) = \frac{1}{\pi} \frac{\operatorname{Im} \Phi_{if}(x)}{[x + nV_{if} - \operatorname{Re} \Phi_{if}(x)]^2 + [\operatorname{Im} \Phi_{if}(x)]^2}, \tag{4}$$

and

$$\Phi_{if}(x) = \frac{-n\int_0^\infty \frac{dV_{if}(t)}{dt}\, e^{-ixt}\int_0^\infty e^{-ixt'}\overline{U}_{if}(t'+t)\,dt'dt}{\int_0^\infty e^{-ixt}\overline{U}_{if}(t)dt}, \tag{5}$$

which will be re-derived in the Appendix I. On the wings of the line, *i. e.* in the limit of large x, the only important contribution to the integral in the numerator of the last formula comes from the vicinity of the initial ($t = 0$) time, so that we arrive at the asymptotic formula

$$\Phi_{if}(x) \cong -n\int_0^\infty \frac{dV_{if}(t)}{dt}\, e^{-ixt}dt, \tag{6}$$

which follows also from the resolvent method in the binary collision approximation.

As it follows from the previous paper and as it will be seen from the present considerations, the function occuring here, namely the function $m_{if}(x)$ defined by

$$m_{if}(x) = \int_0^\infty \frac{dV_{if}(t)}{dt}\, e^{-ixt}dt \tag{7}$$

is of crucial importance for the pressure broadening theory by the dilute gases. Therefore it is desirable to express this function by some quantities of a definite physical meaning like the scattering amplitudes. This problem has been already worked out in the paper of Fano [4]. However, the structure of the solution presented there was extremely complicated. As we shall see here, both the proof and the form of this solution can be greatly simplified. Let us start by introducing the one-perturber eigenfunctions φ_a^- and ψ_b^+ of the Hamiltonians h_i and h_f, *i. e.*

$$h_i\varphi_a^- = \varepsilon_a\,\varphi_a^- \tag{8}$$

and

$$h_f\psi_b^+ = \varepsilon_b^+\psi_b^+, \tag{9}$$

where a and b stand for all the quantum numbers of the one-perturber motion. We shall use the following identity

$$\begin{aligned}(\varphi_a^-, (h_i - h_f)\psi_b^+) = (\varphi_a^-, v_i\chi_b) - (\chi_a, v_f\psi_b^+) + \\ + (\varphi_a^-, v_i(\psi_b^+ - \chi_b)) - ((\varphi_a^- - \chi_a), v_f\psi_b^+),\end{aligned} \tag{10}$$

where χ_a denotes the eigenfunction of the kinetic energy operator k, *i. e.*

$$k\chi_a = \varepsilon_a\chi_a. \tag{11}$$

As yet there was no need to specify the set of functions φ_a^- and ψ_b^+, which are chosen now as the out ingoing waves, *i. e.*

$$\varphi_a^- = \lim_{\eta\to+0} \frac{-i\eta}{\varepsilon_a - h_i - i\eta}, \tag{12}$$

and

$$\psi_b^+ = \lim_{\eta \to +0} \frac{i\eta}{\varepsilon_b - h_f + i\eta}. \tag{13}$$

We will express the function $m_{if}(x)$ by the following quantities

$$\tilde{\mathcal{T}}_{ab}^{(i)} = (\varphi_a^-, v_i \chi_b), \tag{14}$$

and

$$\mathcal{T}_{ab}^{(f)} = (\chi_a, v_f \psi_b^+), \tag{15}$$

which reduce to transition amplitudes on the energy shell. The identity (10) leads now to the following equality

$$(\varphi_a^-, (h_i - h_f)\psi_b^+) = \tilde{\mathcal{T}}_{ab}^{(i)} - \mathcal{T}_{ab}^{(f)} + \int dc \tilde{\mathcal{T}}_{ac}^{(i)} \left[\frac{1}{\varepsilon_b - \varepsilon_c + i0} - \frac{1}{\varepsilon_a - \varepsilon_c + i0} \right] \mathcal{T}_{cb}^{(f)}. \tag{16}$$

This is the solution of our problem since the function $m_{if}(x)$ is, for sufficiently large volume Ω, given by

$$m_{if}(x) = -\lim_{\Omega \to \infty} \Omega \int da \int db \varrho(\varepsilon_a) \frac{|(\varphi_a^-, (h_i - h_f)\psi_b^+)|^2}{x - \varepsilon_a + \varepsilon_b - i0}. \tag{17}$$

The other way of approaching the problem is to observe that the asymptotic formula (6) combined with (4) leads to the following formula

$$J_{if}(x) \simeq n\pi^{-1} x^{-2} \operatorname{Im} m_{if}(x), \tag{18}$$

which holds for sufficiently large x. Using the explicit form (17) of the function $m_{if}(x)$ we arrive at

$$J_{if}(x) \simeq n \int da \int db \varrho(\varepsilon_a) |(\varphi_a^-, \psi_b^+)|^2 \delta(x - \varepsilon_a + \varepsilon_b), \tag{19}$$

which is exactly the formula of Jabłoński [5].

3. *The asymptotic behaviour of the autocorrelation function*

As it is widely recognized, the asymptotic behaviour of the autocorrelation function determines the intensity distribution in the vicinity of the line centre. Although this problem has been already worked out by Baranger [6], it seems desirable to attach a more precise meaning to this statement.

We start with the following asymptotic formula

$$\int_0^t V_{if}(t)dt = (m_{if} + V_{if})t - im'_{if} + \frac{\vartheta}{t} + O\left(\frac{1}{t^2}\right), \tag{20}$$

which is derived in the Appendix II. The coefficient ϑ is determined by the zero energy expansion of the scattering amplitudes in the following way

$$\vartheta = -\frac{i\pi}{8} \int da \int db \varrho(\varepsilon_a) \delta(\varepsilon_a) \delta(\varepsilon_b) \varepsilon_a^{-\frac{1}{2}} \varepsilon_b^{-\frac{1}{2}} |(\varphi_a^-, (h_i - h_f)\psi_b^+)|^2. \tag{21}$$

In order to see how the asymptotic expansion (20) leads to an approximate expression for the intensity distribution function consider first the following integral

$$R(x) = i \int_0^\infty e^{-xt} \overline{U}_{if}(t)\, dt, \tag{22}$$

which is tied to the function $J_{if}(x)$ by the relation

$$J_{if}(x) = \frac{1}{\pi} \operatorname{Im} R(x). \tag{23}$$

Let us decompose this integral into two parts

$$R(x) = i \int_\tau^\infty e^{-ixt} \overline{U}_{if}(t)\, dt + i \int_0^\tau e^{-ixt} \overline{U}_{if}(t)\, dt. \tag{24}$$

The first integral, on the right-hand side of this equality, is estimated by

$$i \int_\tau^\infty e^{-ixt} \overline{U}_{if}(t) dt \approx \frac{\exp\{-i(x+nV_{if}+nm_{if})\tau\}}{x+nV_{if}+nm_{if}} \exp\{im'_{if}|_{x=0}\}, \tag{25}$$

provided that τ is large enough, *i. e.* subjected to the following condition

$$\tau \gg n|\vartheta|. \tag{26}$$

On the other hand, the second term in (24) is majorized by τ, *i. e.*

$$\left| \int_0^\tau e^{-ixt} \overline{U}_{if}(t) dt \right| < \tau, \tag{27}$$

and therefore does not contribute appreciably to $R(x)$, if τ is short enough. Comparing the last inequality with the estimate (25) we arrive at the following condition

$$|x+nV_{if}+nm_{if}|\tau \ll 1. \tag{28}$$

Quite obviously, the last condition and the previous one, namely the strong inequality (26), will be satisfied simultaneously in this case only when the following condition

$$|x+nV_{if}+nm_{if}|n\vartheta \ll 1 \tag{29}$$

is satisfied. Then the function $R(x)$ becomes approximately equal to

$$R(x) \approx \frac{\exp\{inm'_{if}\}}{x+nV_{if}+nm_{if}}. \tag{30}$$

Coming to the end of this discussion we conclude, that the intensity distribution is given as follows

$$J_{if}(x) \approx \frac{1}{\pi} \operatorname{Im} \frac{\exp\{inm'_{if}\}}{x+nV_{if}+nm_{if}}. \tag{31}$$

in the vicinity of the line centre, provided that the density of the gas is subjected to the condition (26) and to the following one

$$n^2 \vartheta \operatorname{Im} m_{if} \ll 1. \tag{32}$$

The centre of the line is defined then as the region where the inequality (29) is satisfied. Neglecting the exponential factor in (31), as unessential for sufficiently low densities, we arrive at the Lorentzian distribution

$$J_{if}(x) \approx -\frac{1}{\pi} \frac{n \operatorname{Im} m_{if}}{[x+nV_{if}+n \operatorname{Re} m_{if}]^2+[n \operatorname{Im} m_{if}]^2}, \tag{33}$$

which is the well-known impact theory result. Still, using the formula (31) we improve the impact theory calculations whenever the interaction between the perturbers may be neglected.

4. The line shape in the binary collision approximation

As yet we have gathered some informations concerning the wings and the centre of line. On the wings, the asymptotic formula (6) combined with the equality (4) and the definition (7) leads to

$$J_{if}(x) \simeq -\frac{1}{\pi} \frac{n \operatorname{Im} m_{if}(x)}{[x+nV_{if}+n \operatorname{Re} m_{if}(x)]^2+[n \operatorname{Im} m_{if}]^2}, \tag{34}$$

according to the formula (33), while in the vicinity of the centre the line shape is Lorentzian for low densities. A remarkable fact is, that the formula (33) follows from (34) provided that $m_{if}(x)$ is nearly constant in the centre of line. Thus, we may suspect, that the formula (34) is approximately valid in the whole frequencies domain if only the density of the gas is low enough. This supposition seems to be confirmed by the analysis of the complex function $\Phi_{if}(x)$. In fact, as is to be seen from the appendix *I*, the function $R(x)$ is related to the function $\Phi_{if}(x)$ by

$$R(x) = [x+nV_{if}-n\Phi_{if}(x)]^{-1}. \tag{35}$$

This relation combined with (5) yields

$$\Phi_{if}(x) = n \int \varepsilon \frac{x+nV_{if}-\Phi_{if}(x)}{x+nV_{if}-\varepsilon-\Phi_{if}(x-\varepsilon)} d\omega_\varepsilon, \tag{36}$$

where the following abbreviation is introduced

$$\int f(\varepsilon)\, d\omega_\varepsilon \equiv \Omega \int da \int db\, \varrho(\varepsilon_a) f(\varepsilon_a-\varepsilon_b) |(\varphi_a^-, \psi_b^+)|^2. \tag{37}$$

Moreover, since

$$\int \varepsilon d\omega_\varepsilon = V_{if}, \tag{38}$$

we find that

$$\Phi_{if}(x) = nV_{if}-n \int \varepsilon \frac{\varepsilon+\Phi_{if}(x-\varepsilon)-\Phi_{if}(x)}{x+nV_{if}-\varepsilon-\Phi_{if}(x-\varepsilon)} d\omega_\varepsilon. \tag{39}$$

Eventually we arrive at the following formula

$$\Phi_{if}(x) = nV_{if} - n \int \varepsilon^2 \frac{1-\delta(x-\varepsilon, x)}{(x+nV_{if}-\varepsilon)\,[1-\delta(x-\varepsilon, 0)]-\Phi_{if}(0)}, \tag{40}$$

where the function $\delta(x_1, x_2)$ is defined by

$$\delta(x_1, x_2) = \frac{\Phi(x_1)-\Phi(x_2)}{x_1-x_2}. \tag{41}$$

If the derivative of the function $\Phi_{if}(x)$ is finite, we can always find a low enough density so that the function $\delta\ (x_1, x_2)$ is negligibly small. Thus we arrive at

$$\Phi_{if}(x) \approx nV_{if} - n \int \frac{\varepsilon^2}{x+nV_{if}-\varepsilon-\Phi_{if}(0)}\, d\omega_\varepsilon, \tag{42}$$

or at the formula (6) for the dilute gases. In both cases we work within the binary collision approximation. However, using the formula (42) we improve our calculation provided that the interaction between the perturbers is really negligible. Near the centre of the line the last formula leads to the following estimate

$$\Phi_{if}(x) \approx nV_{if} - nm_{if} - m'_{if}(x+nV_{if}-nm_{if}), \tag{43}$$

which, when substituted into (4), confirms the previously deduced intensity distribution (31).

5. The numerical results

5.1. The impact theory calculation

The low density measurements of the line shift and half-width ensures the possibility of fixing the potential constants, if only we have chosen a two-parameter interatomic potential. We will require such a potential to display some resemblance to the "true" interatomic potential, thus it shall increase rapidly at short and decrease according to the inverse sixth power law at long distances. Since the long-range part of the potential may be calculated very accurately in an independent way, we are in position to verify our results. However, the experience of Hindmarsh and others [7] is rather disappointing. They have used one of the potentials of the Lennard-Jones family, which are generally given by the following formula

$$V[R] = -\varepsilon_m \left\{ \frac{6}{n-6} \left(\frac{R_m}{R}\right)^n - \frac{n}{n-6} \left(\frac{R_m}{R}\right)^6 \right\}, \tag{44}$$

where R_m is the position of the potential minimum and ε_m is its value at this point while n is, in principle, any natural number higher than 6 but equal 12 in the quoted paper. The discrepancy of the theory and experiment is not likely to be removed even if some other potentials are tested. In fact, the numerical results gathered by us for the Lennard-Jones potentials with $n = 8$, 10 and 12, which are presented in Figs 1 and 2, indicate that the dependence of the theoretical line shift and half-width on the potential parameters is in

all these cases given by similar and closely situated curves. Even the following modification of the well-known Buckingham potential, namely

$$V[R] = \begin{cases} -\varepsilon_m \left[\exp\left\{ -6 \left[\left(\frac{R}{R_m} \right)^2 - 1 \right] \right\} - 2 \left(\frac{R_m}{R} \right)^6 \right], & R \geqslant \frac{2}{3} R_m \\ -\infty \qquad\qquad\qquad\qquad\qquad\qquad , & R < \frac{2}{3} R_m \end{cases} \tag{45}$$

leads to similar results. Let us note that we have modified here the scale of the variables,

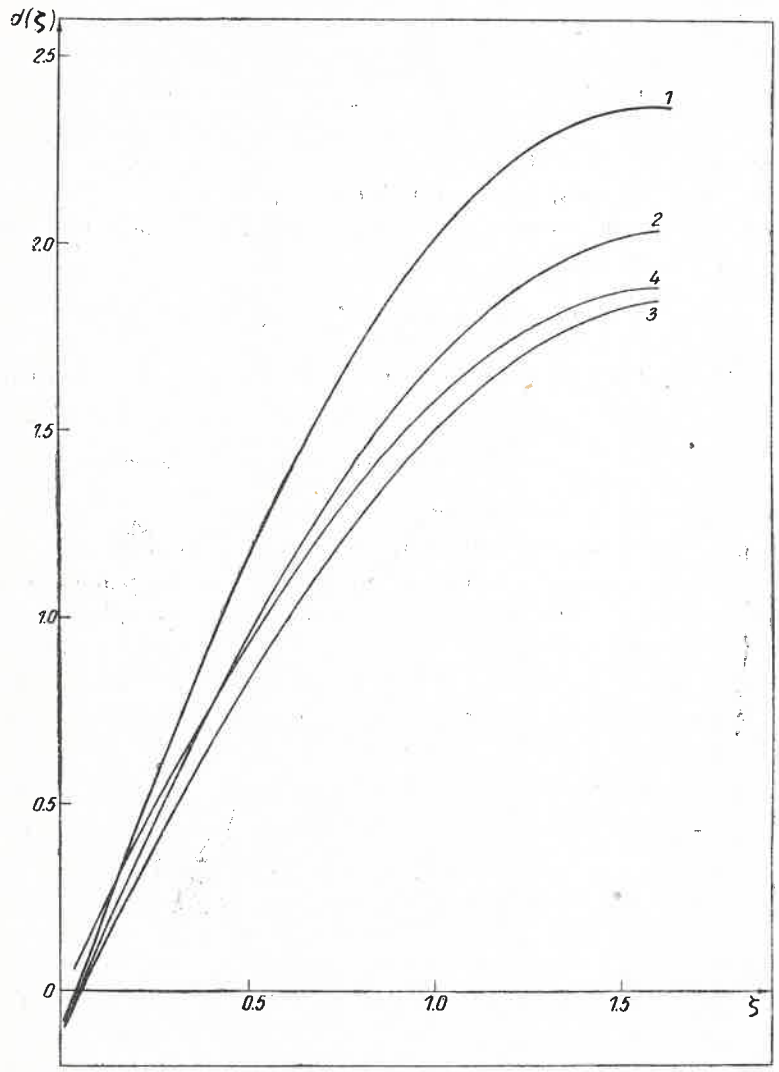

Fig. 1. Line-shift function $d(\zeta)$ calculated with: *1* — *L–J* ($n = 8$) potential, *2* — *L–J* ($n = 10$) potential, *3* — *L–J* ($n = 12$) potential, *4* — potential defined by (45)

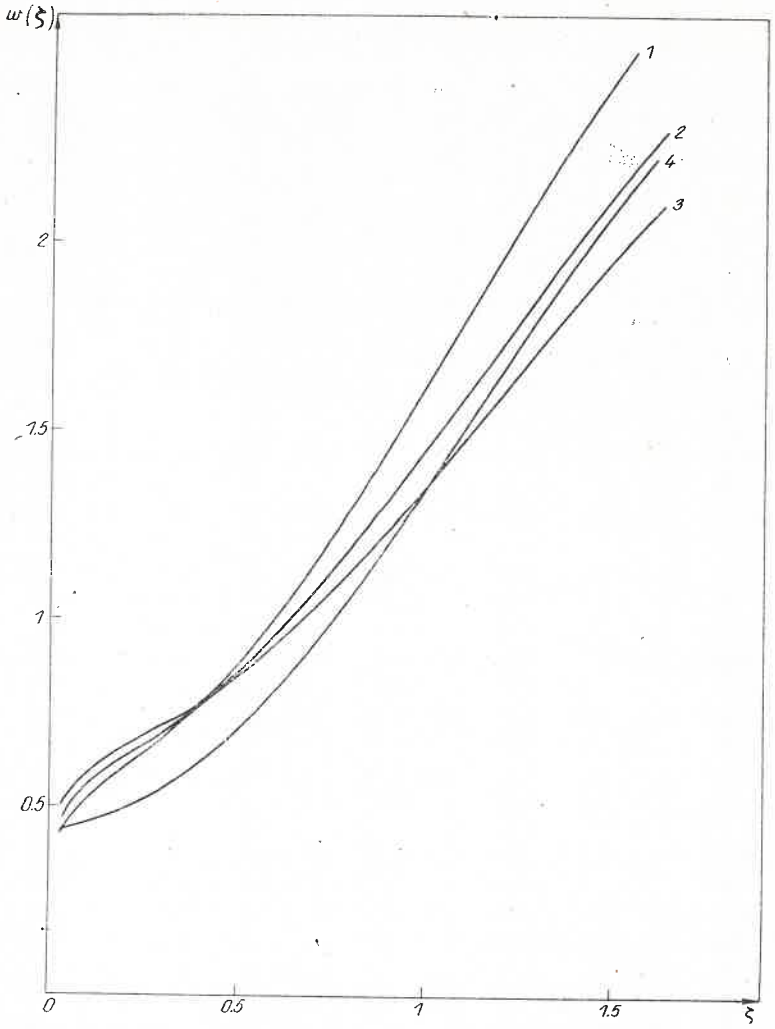

Fig. 2. Half-width function $w(\zeta)$ calculated with the different potentials as in Fig. 1

which have been introduced in the paper I, by substituting the parameters ε_m and R_m for ε_0 and R_0, respectively. Thus we are using here the following definitions

$$J_{if}(x) = \frac{R_m}{\bar{v}} j_{if}(\xi, \zeta, N_0), \tag{46}$$

and

$$\xi = \frac{xR_m}{\bar{v}}, \qquad \zeta = \frac{\varepsilon_m R_m}{\bar{v}h}, \qquad N_0 = \pi n R_m^3. \tag{47}$$

This set of variables is most suitable in comparing the theoretical line shapes resulting from the acceptance of the different potentials. We would like to emphasize that our results are

in complete agreement with those of Hindmarsh and others [7] and that those presented in the paper I for the $L-J$ ($n = 8$) potential have been also confirmed by an independent programme. The programme of our calculation included its refinement by averaging over the Maxwellian distribution of the velocities instead of using, as usually, the mean velocity.

TABLE I

The values of the parameters $d(\zeta)$ and $w(\zeta)$ for different potentials

	$w(\zeta)$				$d(\zeta)$			
ζ	$L-J$ $n=8$	$L-J$ $n=10$	$L-J$ $n=12$	The potential defined by (45)	$L-J$ $n=8$	$L-J$ $n=10$	$L-J$ $n=12$	The potential defined by (45)
0.00[1]	0.263	0.278	0.327		−0.009	−0.019	−0.017	
0.005	0.276	0.316	0.361		−0.046	−0.082	−0.077	
0.01	0.311	0.389	0.429		−0.079	−0.099	−0.097	
0.015	0.355	0.428	0.471		−0.088	−0.073	−0.075	
0.02	0.395	0.436	0.479	0.444	−0.076	−0.059	−0.057	0.038
0.025	0.421	0.451	0.489	0.445	−0.053	−0.059	−0.057	0.048
0.3	0.432	0.474	0.501	0.445	−0.030	−0.048	−0.051	0.057
0.035	0.436	0.484	0.524	0.445	−0.013	−0.029	−0.035	0.067
0.04	0.440	0.488	0.527	0.446	−0.003	−0.020	−0.022	0.077
0.045	0.449	0.499	0.534	0.446	+0.002	−0.014	−0.017	0.086
0.050	0.462	0.512	0.547	0.447	0.011	0.000	−0.009	0.096
0.060	0.486	0.520	0.556	0.448	0.044	+0.023	+0.016	0.115
0.080	0.501	0.543	0.577	0.451	0.099	0.068	0.055	0.153
0.10	0.527	0.563	0.594	0.455	0.158	0.113	0.095	0.191
0.20	0.607	0.635	0.659	0.495	0.426	0.337	0.287	0.395
0.30	0.682	0.697	0.713	0.550	0.677	0.549	0.476	0.570
0.40	0.779	0.774	0.778	0.620	0.922	0.750	0.655	0.755
0.50	0.885	0.861	0.854	0.705	1.150	0.942	0.826	0.914
0.60	1.012	0.959	0.938	0.812	1.361	1.119	0.984	1.074
0.70	1.149	1.071	1.031	0.934	1.555	1.284	1.132	1.221
0.80	1.301	1.191	1.133	1.067	1.728	1.434	1.268	1.355
0.90	1.460	1.320	1.244	1.209	1.882	1.566	1.391	1.475
1.00	1.626	1.454	1.360	1.356	2.011	1.683	1.499	1.580
1.10	1.796	1.592	1.479	1.510	2.122	1.783	1.593	1.669
1.20	1.967	1.733	1.600	1.662	2.209	1.865	1.674	1.742
1.30	2.129	1.871	1.723	1.812	2.277	1.932	1.741	1.800
1.40	2.288	2.007	1.844	1.957	2.324	1.982	1.793	1.842
1.50	2.441	2.139	1.962	2.095	2.359	2.017	1.832	1.869
1.60	2.582	2.263	2.075	2.225	2.369	2.039	1.860	1.884
1.80	2.797	2.465	2.265	2.448	2.340	2.029	1.864	1.877
2.00	3.012	2.667	2.456	2.618	2.311	2.018	1.869	1.835
2.20	3.137	2.800	2.592		2.259	1.972	1.838	
2.40	3.204	2.885	2.688		2.211	1.921	1.794	
2.60	3.228	2.929	2.746		2.187	1.881	1.755	
2.80	3.220	2.939	2.772		2.200	1.863	1.727	
3.00	3.198	2.925	2.771		2.254	1.874	1.721	

If we denote the Maxwellian averaged line shift and half-width parameters by $\bar{d}(\zeta)$ and $\bar{w}(\zeta)$, respectively, then we may relate them, using the definitions (47), in the following way

$$\bar{d}(\zeta) = \sqrt{\frac{54}{\pi}} \int_0^\infty \exp\left\{-\frac{3}{2}\left(\frac{\zeta}{z}\right)^2\right\} z^{-5} d(z) dz, \tag{48}$$

and

$$\bar{w}(\zeta) = \sqrt{\frac{54}{\pi}} \int_0^\infty \exp\left\{-\frac{3}{2}\left(\frac{\zeta}{z}\right)^2\right\} z^{-5} w(z) dz \tag{49}$$

to the corresponding quantities $d(\zeta)$ and $w(\zeta)$, which has been determined previously by the standard methods of the impact theory. In Fig. 3 we show the results of the calculation of $\bar{d}$ and $\bar{w}$ with the help of the last formulas and the functions $\bar{d}$ and $\bar{w}$ known, in the broad

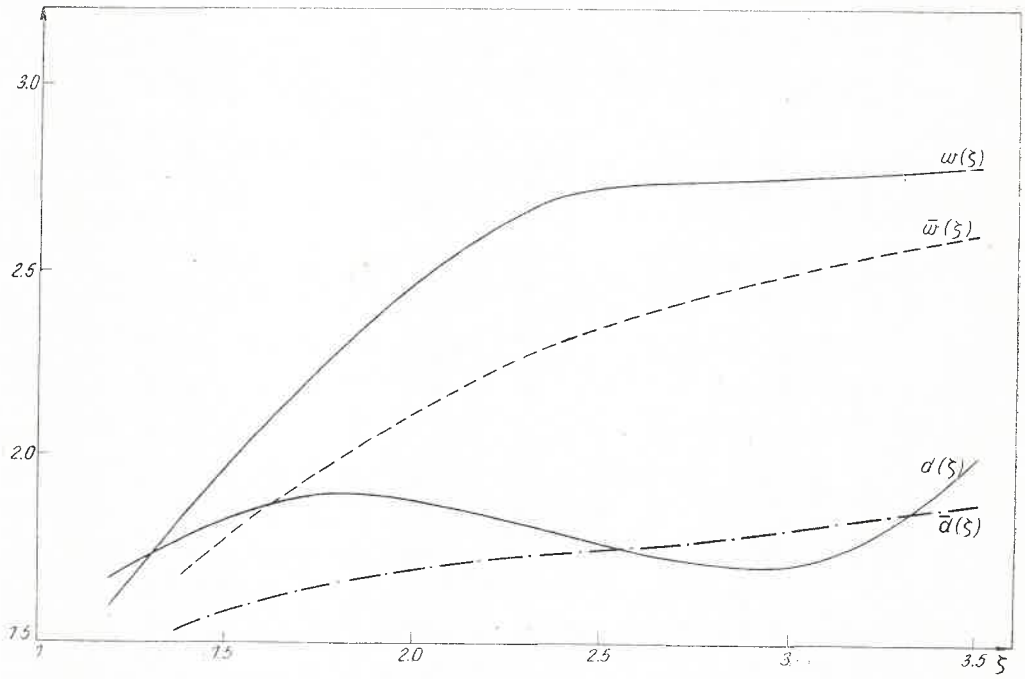

Fig. 3. Function $\bar{d}(\zeta)$ and $\bar{w}(\zeta)$ compared against functions $d(\zeta)$ and $w(\zeta)$ for the L–J ($n = 12$) potential

range of their arguments, from the paper [7] for the $L-J$ ($n = 12$) potential. Knowing $\bar{d}$ and $\bar{w}$ we are in position to estimate the intensity distribution from the formula

$$j_{if}(\xi, \zeta, N_0) \approx \frac{1}{\pi} \frac{N_0 \overline{w(0, \zeta)}}{[\xi - N_0 \overline{d(0, \zeta)}]^2 + [N_0 \overline{w(0, \zeta)}]^2}, \tag{50}$$

which is valid in the impact approximation. It is evident from the diagram of Fig. 3 that

averaging over the Maxwellian distribution we get more smooth curves with a monotonic dependence of the line shift and half-width on ζ.

As it is evident from the definitions (47) the parameter ζ is, for fixed ε_m and R_m, proportional to the inverse of the mean velocity. Thus the parameters $\bar{d}$ and $\bar{w}$ slowly decrease with increasing temperature. The line shift per unit density δ and the corresponding half-width γ are related to $\bar{d}$ and $\bar{w}$ by

$$\delta = \frac{\bar{v}}{R_m}\bar{d}, \qquad \gamma = 2\frac{\bar{v}}{R_m}\bar{w} \tag{51}$$

so that, in the final effect, these parameters reveal a rather weak dependence on temperature.

5.2. The extended binary collision approximation

We have based the calculation of the line shape on the formula (31), which is valid, according to our estimates, in the intermediate pressure range. In the dimensionless variables this formula becomes

$$j_{if}(\xi, N_0) \approx \frac{N_0}{\pi}\left(\frac{w(0) - N_0 d'(0)w(0) + w'(0)\xi + N_0 w'(0)d(0)}{[\xi + N_0 d(0)]^2 + [N_0 w(0)]^2}\right), \tag{52}$$

where the frequency derivatives d' and w' of the functions d and w are given, in the classical path approximation, by the following formulas

$$d'(\zeta, \xi)|_{\xi=0} = 2\zeta^2 \int_{\varrho_0}^{\infty} \varrho d\varrho \int_{-\infty}^{\infty} dz \int_{z}^{\infty} ds u(\varrho, s)u(\varrho, z)[s-z] \times$$
$$\times \cos\left[\zeta \int_{z}^{s} u(\varrho, s')ds'\right], \tag{53}$$

and

$$w'(\zeta, \xi)|_{\xi=0} = -2\zeta^2 \int_{\varrho_0}^{\infty} \varrho d\varrho \int_{-\infty}^{\infty} dz \int_{z}^{\infty} ds u(\varrho, s)u(\varrho, z)]s-z] \times$$
$$\times \sin\left[\zeta \int_{z}^{s} u(\varrho, s')ds'\right], \tag{54}$$

where $u(\varrho, s)$ is the corresponding potential in the dimensionless variables, which is related o the potential $V[R]$ by

$$u(\varrho, s) = \frac{R_m}{\bar{v}h} V[R(\varrho^2 + s^2)^{\frac{1}{2}}]. \tag{55}$$

We do not attempt yet to compare quantitatively the theory with experiment since the low pressure measurements do not seem to be sufficiently accurate. Still the results presented in Figs 4 and 5 are in agreement with those obtained experimentally by Ch'en and Garrett [3] in this sense, that the experimental as well as the theoretical curves show, in the intermediate pressure range, an increasing absolute value of the line shift and half-

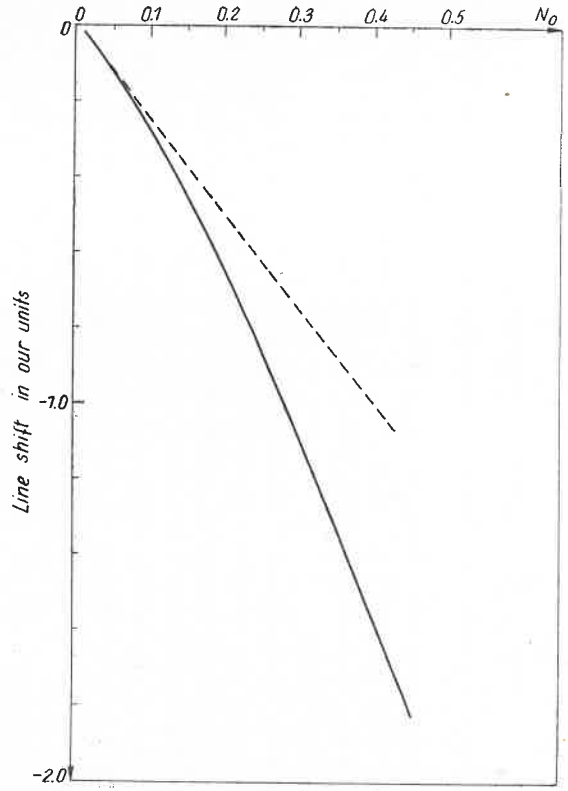

Fig. 4

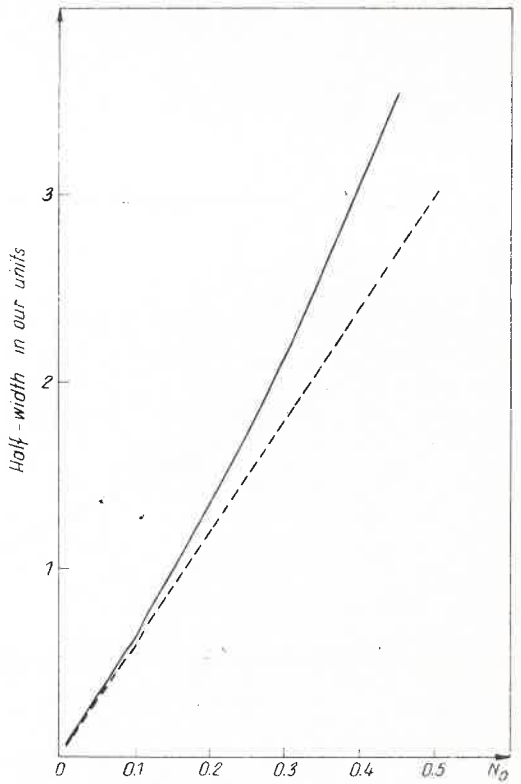

Fig. 5

Fig. 4. Dependence of line shift on pressure following from the formula (52) with L–J potential ($n = 8$) and $\zeta = 2.1$. Dotted line corresponds to impact theory approximation

Fig. 5. Dependence of half-width on pressure following from formula (52). Dotted line corresponds to impact theory approximation

-width per unit pressure parallelly to the increase of the pressure. Moreover, both the calculated and measured asymmetry coefficients, *i.e.* the ratio of the red semi-half-width to the violet one, are rapidly growing with increase of the pressure. The value of ζ used in our calculations is, according to our estimates, close to the one appropriate for the description

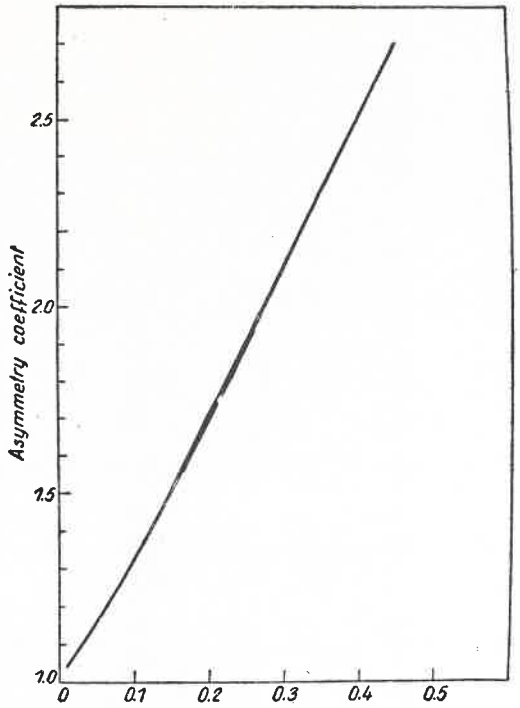

Fig. 6. Dependence of the asymmetry coefficient on pressure following from formula (52)

of the cesium resonance line broadening by argon. The extent of the difference between the Lorentzian line shape ensuing from the impact theory and this resulting from the formula (52) is illustrated in Fig. 7, where the corresponding line shapes are compared for a pressure from the intermediate region.

We have attempted the calculation of the function $w(\xi, \zeta)$, which is, in fact, the imaginary part of $m(x)$ expressed in our units in a manner which should be self-evident. The results are presented, for the $L-J$ ($n = 8$) potential, in Fig. 8, where $w(\xi, \zeta)$ is plotted as a function of the frequency ξ for a given potential constant ζ. Since this function diminishes for large ξ in a manner close to exponential decrease, the intensity distribution function, given by the formula (18), decreases rapidly on the wings. After the function $w(\xi, \zeta)$ as well as the function $d(\xi, \zeta)$ is calculated, we may determine the line shape, which follows from the formula

$$j_{if}(\xi, \zeta, N_0) = \frac{1}{\pi} \frac{N_0 w(\xi, \zeta)}{[\xi - N_0 d(\xi, \zeta)]^2 + [N_0 w(\xi, \zeta)]^2} \tag{56}$$

known from the paper I and corresponding to the results of the resolvent operator method (Fano [4]). As an example we have compared, in Fig. 9, such a line shape with the correspond-

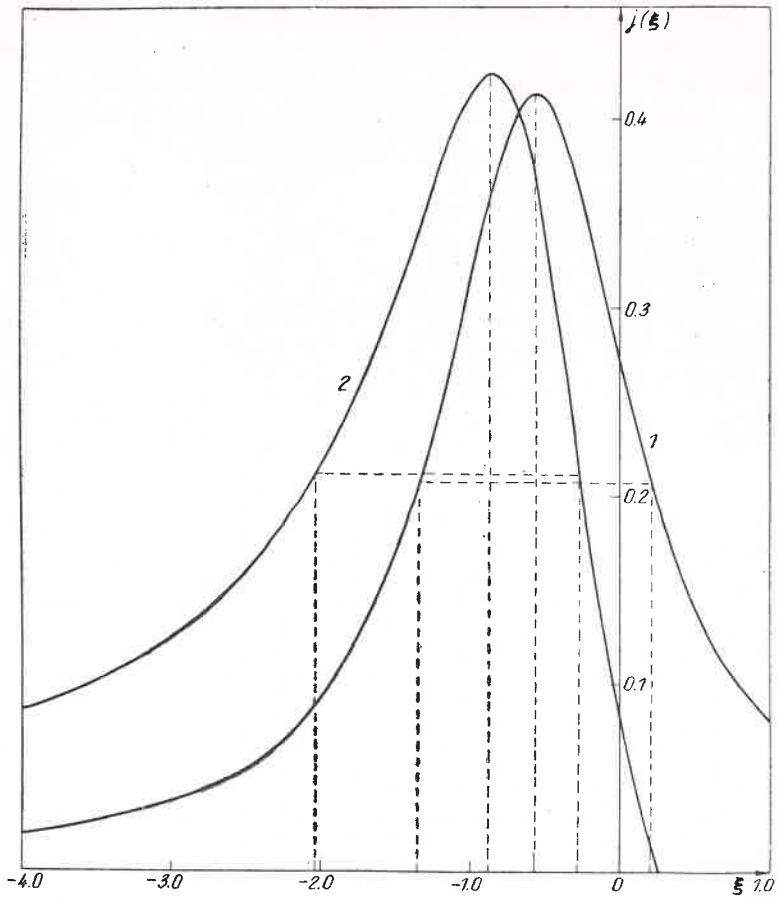

Fig. 7. Lorentzian profile (*1*) compared against curve (*2*) resulting from formula (52), ($N_0 = 0.25$)

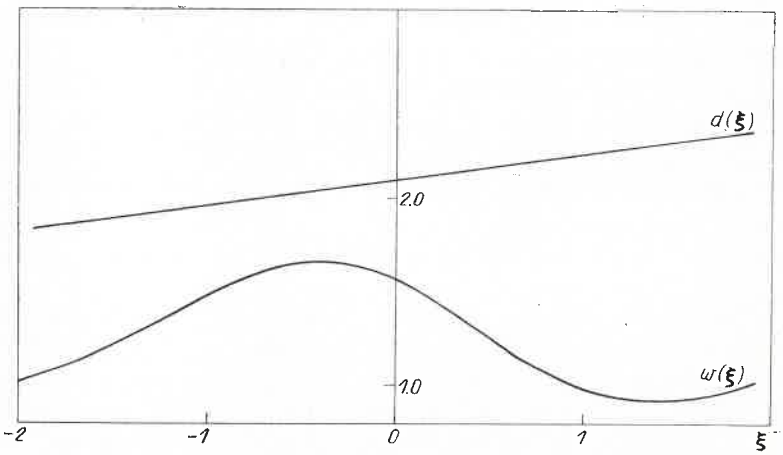

Fig. 8. Functions $d(\xi, \zeta)$ and $w(\xi, \zeta)$ plotted for L–J ($n = 8$) potential with $\zeta = 0.7$

ing profile resulting from the formula (52). The difference between these profiles is important in the intermediate pressure range, where the formula proposed in the present paper seems to be more close to the experimental evidence.

We are indebted to our Colleagues from the computing centre, especially to Dr A. Schurmann, for their contribution to the numerical calculations.

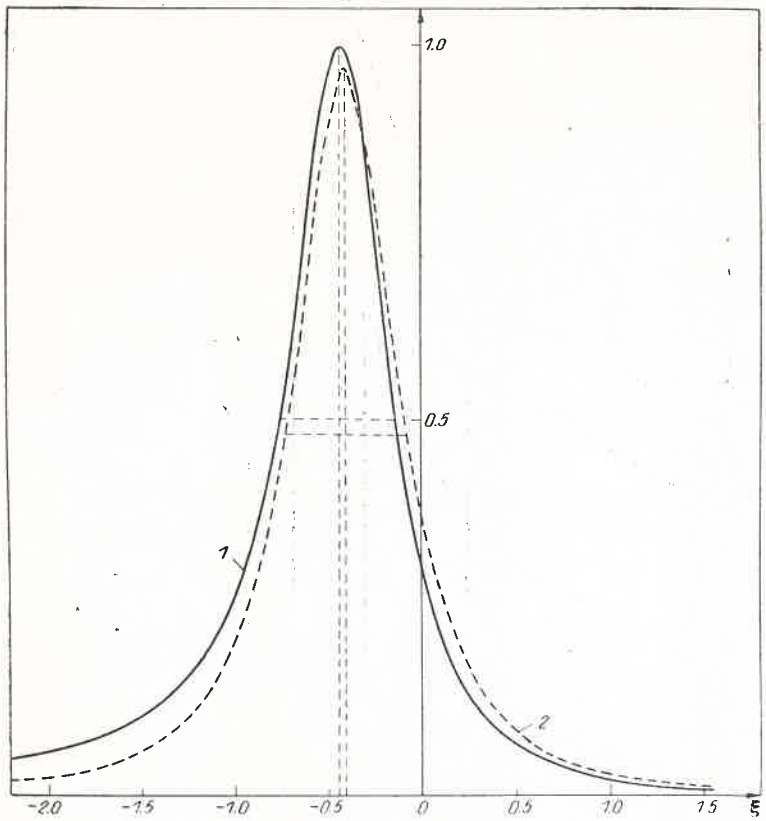

Fig. 9. Profiles resulting from formula (52) (curve *1*) and formula (56) (curve *2*), ($N_0 = 0.2$)

APPENDIX I

We will derive here the formula (4) starting from the differential equation

$$i\frac{d\overline{U}_{if}(t)}{dt} = nV_{if}(t)\overline{U}_{if}(t), \tag{AI.1}$$

which follows immediately from (1). Multiplying both sides of this equation by the factor $\exp(-ixt)$ and performing the time integration we arrive at

$$n\int_0^\infty e^{-ixt}V_{if}(t)\overline{U}_{if}(t)dt = i\int_0^\infty e^{-ixt}\frac{d\overline{U}_{if}(t)}{dt}\,dt = -i-x\int_0^\infty e^{-ixt}\overline{U}_{if}(t)dt. \tag{AI.2}$$

This formula, on account of the definition (22), yields

$$R(x) = x^{-1} - nx^{-1}i \int_0^\infty e^{-ixt} V_{if} \overline{U}_{if}(t)(t)dt. \tag{AI.3}$$

Finally, if we adopt the formula (5) as the definition of the function $\Phi_{if}(x)$, we obtain the following relation

$$R(x) = x^{-1} + x^{-1}(\Phi_{if}(x) - nV_{if})R(x), \tag{AI.4}$$

from which we get the relation (35). These basic formula (4) follows then from the equation (23), which is a simple consequence of (3) and the definition (22) of the function $R(x)$

APPENDIX II

In order to find the asymptotic formula (20) let us start from the following identity

$$\int_0^t V_{if}(t')dt' = \int_0^t (t-t') \frac{dV_{if}(t')}{dt'} dt' + tV_{if}. \tag{AII.1}$$

Moreover, let us observe that

$$\int_0^\infty \frac{dV_{if}(t')}{dt'} dt' = m_{if}, \tag{AII.2}$$

and

$$\int_0^\infty t' \frac{dV_{if}(t')}{dt'} dt' = i \lim_{x \to 0} \frac{d}{dx} \int_0^\infty e^{-ixt'} \frac{dV_{if}(t')}{dt'} dt' = im'_{if} \tag{AII.3}$$

where m_{if} and m'_{if} are the values of the function $m_{if}(x)$ and its derivative at the frequency of the unperturbed line ($x = 0$). Now the identity (AII.1) leads to

$$\int_0^t V_{if}(t')dt' = (m_{if} + V_{if})t - im'_{if} - \int_t^\infty (t-t') \frac{dV_{if}(t')}{dt'} dt'. \tag{AII.4}$$

The further analysis will be based on the asymptotic formula

$$\int_0^\infty \varepsilon^{-\frac{1}{2}} g(\varepsilon) e^{\pm i\varepsilon t} d\varepsilon = \frac{\Gamma(\frac{1}{2})}{t^{\frac{1}{2}}} e^{\pm \frac{\pi}{4} i} g(0) + 0\left(\frac{1}{t}\right), \tag{AII.5}$$

which holds in the function $g(\varepsilon)$ is finite in the whole interval $(0, \infty)$ of ε and if it vanishes at infinity (see *e.g.* Copson [8]). What we need now is the explicit form of the derivative of the function $V_{if}(t)$, which is

$$\frac{dV_{if}(t)}{dt} = -i \int da \int db \varrho(\varepsilon_a) |(\varphi_a^-, (h_i - h_f)\psi_b^+)|^2 e^{-i(\varepsilon_a - \varepsilon_b)t}, \tag{AII.6}$$

as it follows directly from the definition (2). We presume that this expression may be put in the form of

$$\frac{dV_{if}(t)}{dt} = -i\int_0^\infty d\varepsilon_a \int_0^\infty d\varepsilon_b \varepsilon_a^{-\frac{1}{2}}\varepsilon_b^{-\frac{1}{2}}\gamma(\varepsilon_a, \varepsilon_b)\exp\{-i(\varepsilon_a-\varepsilon_b)t\}, \tag{AII.7}$$

where the function $\gamma(\varepsilon_a, \varepsilon_b)$ satisfies, with respect to the energies ε_a and ε_b separately, the conditions for the formula (AII.5) to be hold. This assumption is justified, since the transition amplitudes tend to constant when the energy approaches zero (see *e.g.* Goldberger and Watson [9]) and the densities of the energy states are proportional to the square root of the corresponding energies. Quite obviously, we do not take into account the possible resonances.

The formula (AII.5), when applied to (AII.7), yields

$$\frac{dV_{if}(t)}{dt} = -\frac{i}{t^3}\frac{\pi}{4}\gamma(0, 0)+O\left(\frac{1}{t^4}\right). \tag{AII.8}$$

Finally, we arrive at

$$\frac{dV_{if}(t)}{dt} = -\frac{i}{t^3}\frac{\pi}{4}\int da\int db\varrho(\varepsilon_a)\delta(\varepsilon_a)\delta(\varepsilon_b)\frac{|(\varphi_a^-, (h_i-h_f)\psi_b^+)|^2}{\sqrt{\varepsilon_a}\sqrt{\varepsilon_b}}+O\left(\frac{1}{t^4}\right), \tag{AII.9}$$

which, when combined with (AII.4), leads to the asymptotic expansion (20) with ϑ given by (21).

REFERENCES

[1] J. Fiutak, E. Czuchaj, *Acta Phys. Polon.*, **A37**, 85 (1970).
[2] H. R. Griem, M. Baranger, A. C. Kolb, G. Oertel, *Phys. Rev.*, **125**, 177 (1962).
[3] S. Y. Ch'en, R. O. Garrett, *Phys. Rev.*, **144**, 59 (1966).
[4] U. Fano, *Phys. Rev.*, **131**, 259 (1963).
[5] A. Jabłoński, *Phys. Rev.*, **68**, 78 (1945).
[6] M. Baranger, *Phys. Rev.*, **111**, 494 (1958).
[7] W. R. Hindmarsh, A. D. Petford, G. Smith, *Proc. Roy. Soc.*, **A297**, 296 (1967).
[8] E. T. Copson, *Asymptotic Expansions*, Cambridge University Press, Cambridge 1965.
[9] M. L. Goldberger, K. M. Watson, *Collision Theory*, John Wiley and Sons, Inc., New York — London — Sydney 1964.